DOCTORAL DISSERTATION SERIES
Publication No.: 12, 637

AUTHOR: Raymond Bradley Roof, Jr., Ph. D., 1955
University of Michigan

TITLE: THE CRYSTAL STRUCTURE OF FERRIC ACETYLACETONATE, AN APPLICATION OF FOURIER SERIES TO CRYSTAL STRUCTURE ANALYSIS

University Microfilms, Ann Arbor, Michigan

THE CRYSTAL STRUCTURE OF FERRIC ACETYLACETONATE, AN APPLICATION OF FOURIER SERIES TO CRYSTAL STRUCTURE ANALYSIS

by RADLEY
Raymond B. Roof, Jr.

A dissertation submitted in partial fulfillment
of the requirements for the degree of
Doctor of Philosophy in the
University of Michigan
1955

Doctoral Committee:

Professor Lewis S. Ramsdell, Chairman
Assistant Professor Reynolds M. Denning
Associate Professor Maurice J. Sinnott
Professor Chester B. Slawson
Professor Lars Thomassen

THE CRYSTAL STRUCTURE OF FERRIC ACETYLACETONATE, AN APPLICATION OF FOURIER SERIES TO CRYSTAL STRUCTURE ANALYSIS

by
Raymond B. Roof, Jr.

The crystal structure of ferric acetylacetonate, $Fe(C_5H_7O_2)_3$, has been determined from its X-ray diffraction pattern.[2] The crystals are orthorhombic with a = 15.471, b = 13.577, and c = 16.656 A. The unit cell contains eight molecules and the space group is Pbca. The trial structure was deduced by use of Harker sections, Patterson projections, and electron density projections. The Harker sections were used to find the position of the Fe atom. Patterson projections were used to determine the orientation of the $Fe-O_6$ octahedron. Electron density projections were used to distinguish between the various ways the carbon atoms can be attached to the $Fe-O_6$ octahedron. The approximate atomic coordinates were refined by a bounded projection of a partial three-dimensional Fourier summation, utilizing 775 experimental structure amplitudes.

The experimental structure factors were fitted to an anisotropic temperature factor. X-rays which have been reflected from one set of planes may be reflected from another set of lattice planes which happen, by chance, to be in the correct orientation. These reflections are termed "double" reflections. By use of an anisotropic temperature factor and the identification of "double" reflections the following interatomic distances were calculated; Iron-Oxygen 1.96 ± 0.016, Oxygen-Carbon 1.27 ± 0.022, Carbon-Carbon 1.39 ± 0.023, and Carbon-Carbon 1.54 ± 0.023 A. The iron-oxygen distance found is less than the normal ionic distance and explains the non-ionic properties of the compound as well as the relatively large stability of the molecule. The assumed octahedral character of the iron atom was confirmed as was the dynamic coordination complex model proposed for the organic radical.

Intermolecular contacts are of an order signifying very weak Van der Waals forces. The closest approach of terminal carbon atoms between molecules is 3.78 A. for molecules related by the a glide, 4.12 A. for molecules related by the b glide, and 5.08 A. for molecules related by the c glide.

The crystal structure of ferric acetylacetonate thus consists of discrete molecules linked together in layers by weak van der Waals forces.

ACKNOWLEDGEMENTS

The writer wishes to express his gratitude to Dr. L. S. Ramsdell for his interest and helpful suggestions throughout the investigation.

Acknowledgement is made to Dr. J. H. Norman of the University of Wisconsin for the initial preparation of the compound and to Mr. J. L. Roof of Farnsworth Electronics Co. for the design of the electronic portion of the microphotodensitometer.

The Office of Naval Research supplied funds for the construction of the microphotodensitometer.

TABLE OF CONTENTS

Introduction	1
Crystallization and Morphology	3
Unit Cell and Space Group	4
Intensity Measurements	6
Determination of the Trial Structure	10
Refinements of Atomic Coordinates	21
Location of Hydrogen Atoms	28
Evaluation of the Residual	30
The Accuracy of the Determination	39
Description of the Structure	43
Appendix I Observed and Calculated Structure Factors	50
Appendix II Electronic Circuits for a Microphotodensitometer	53
Bibliography	62

LIST OF TABLES

Table 1:	Comparison of Preliminary Data	5
Table 2:	Conditions for Evaluation of the Residual	32
Table 3:	Final Atomic Coordinates for One Molecule	44
Table 4:	Coordinates of Hydrogen Atoms (Calculated)	45
Table 5:	Legend for Figure 13	56

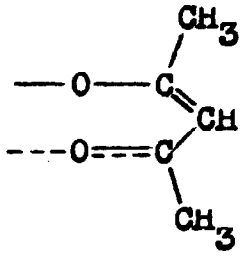
LIST OF ILLUSTRATIONS

Figure 1:	Harker Sections	12
Figure 2:	Patterson Projections	14
Figure 3:	Electron Density Projection on (001)	17
Figure 4:	Reflections for hkl	19
Figure 5:	Final Orientation of the Molecule	26
Figure 6:	General Geometrical Conditions for "Double" Reflection of X-rays	34
Figure 7:	F_c/F_o vs. $\sin^2\theta$	37
Figure 8:	Variation of B with Angle	38
Figure 9:	Electron Density vs. r^2	41
Figure 10:	Ferric Acetylacetonate	46
Figure 11:	Structure Projected on (001)	47
Figure 12:	Structure Projected on (010)	48
Figure 13:	Circuit for Measurement of Very Small Values of Illumination	55
Figure 14:	Circuit for Power Supply	57
Figure 15:	Multiple Meter Ranges Details	58

INTRODUCTION

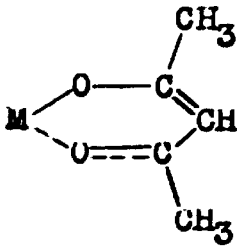
In recent work at the University of Wisconsin on the relative strengths of chelating agents the compound ferric acetylacetonate, $Fe(C_5H_7O_2)_3$, was prepared. Routine examination at the University of Michigan revealed a unit cell and space group different from those reported by Astbury (1926). With this new information Weissenberg photographs and Fourier analysis were used to determine a new crystal structure for the compound. Weissenberg photographs and Fourier analysis are more effective techniques than those used by Astbury; namely, rotation photographs and facial development of the crystals. The time of Astbury's work, 1926, was almost pre-Weissenberg and the techniques of Fourier analysis were not well developed then.

Morgan (1926) has shown that the metallic acetylacetonates cannot be considered as simple metallic salts or an organic acid. They are internal metallic complexes or a unitary type with the central metallic atom so closely associated in the organic radical of the molecule that the metallic atom no longer has ion properties which are used for its detection in qualitative chemical analysis. In accounting for the exceptional properties of the acetylacetonates of the metals, Morgan assumed that the acetylacetonate radical, $C_5H_7O_2$, was a chelate group which functioned in coordination complexes as a two-fold associating unit. Thus,



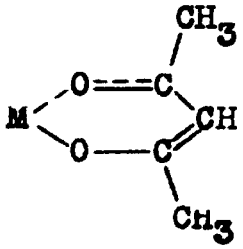
This formula can be regarded as a dynamic one so that the ring completed by the addition of the central metal atom, M, can be considered to oscillate between two extreme positions. Thus,

I

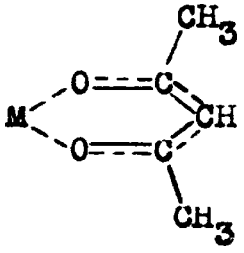


and

II



The average between these two extremes results in



which gives the ring system a plane configuration and a plane of symmetry. Also, since the metallic acetylacetones are relatively stable, the stability has been assumed to be due to a symmetrical arrangement of the chelate groups around the central metallic atom. For the case at hand this means the arrangement of six oxygen atoms in octahedral coordination around the central iron atom.

CRYSTALLIZATION AND MORPHOLOGY

Crystals of ferric acetylacetonate were prepared in the following manner. Washed ferric hydroxide, which has been freshly precipitated, was treated with acetylacetone in slight excess. Ferric acetylacetonate precipitated. This was filtered and recrystallized from ether. The color of the crystals is blood-red, and they occur as orthorhombic tabular crystals with {001}, {210}, and {010} predominating.

Astbury (1926) reports the following goniometric measurements; $(010)\wedge(210) = 60°22'$ and $(210)\wedge(2\bar{1}0) = 59°16'$. The writer's measurements are in excellent agreement with the above; $(010)\wedge(210) = 60°22' \pm 2'$ and $(210)\wedge(2\bar{1}0) = 59°16' \pm 5'$.

Cleavage is perfect, parallel with {010}, and good, parallel with {210}. Optical data, obtained by immersion methods, are

$\alpha = 1.657$ Sign (-)
$\beta = 1.666$
$\gamma = 1.670$ $2V = 69°$ (calc.)

These values are for room temperature and for red light of approximately 620 mμ. The mean value of the transmitted red band passed by the crystal is 620 mμ as determined by a wedge interference filter. The orientation of the biaxial indicatrix is α, β, and γ parallel to the c, b, and a axes, respectively, of the orthorhombic system. The plane of the optic axes is (010).

UNIT CELL AND SPACE GROUP

Table 1 compares the unit cell dimensions and other data as reported by Astbury (1926) with the results obtained by the writer.

In the present work Iron radiation was used both for the determination of the unit cell dimensions and for intensity data. The lattice constants of ferric acetylacetonate were calculated from 0-level Weissenberg photographs, and Bradley & Jay's (1932) extrapolation procedures were employed. The X-ray camera was calibrated by use of 0-level Weissenberg photographs of a NaCl crystal. The density of ferric acetylacetonate was determined by use of a Berman torsion balance utilizing mineral oil with S.G. = 0.881 as the immersion liquid. Observed extinctions are {0k\} for k odd, {h0\} for \ odd, and {hk0} for h odd; from which the space group is unambiguously determined as P<u>bca</u>.

TABLE 1

Comparison of Preliminary Data

Astbury (1926)	Roof
Unit Cell a_o = 15.74 Å. b_o = 13.68 c_o = 33 (?)	 a_o = 15.471 ± 0.002 Å. b_o = 13.577 ± 0.002 c_o = 16.656 ± 0.002
Density ρ = 1.33	 ρ = 1.31 (Experimental) ρ = 1.34 (X-rays)
Molecules per unit cell Z = 16	 Z = 8
Space Group Orthorhombic Pnma	 Orthorhombic Pbca

INTENSITY MEASUREMENTS

In order to obtain an accurate relative intensity scale, the following procedure was used. Before each Weissenberg level exposure, a calibration strip of film was cut from the Weissenberg film. After the Weissenberg level exposure was completed the calibration strip of film was placed in the X-ray camera, and an arbitrary amount of X-rays was allowed to strike the strip for various amounts of time. The Weissenberg level and the calibration strip were then developed together. During development the developing solution was agitated periodically. The calibration strip thus establishes an experimental density vs. exposure curve for the individual level.

In order to measure accurately the density of the calibration strip and the Weissenberg level, a microphoto-densitometer device was constructed. Details of the device are described in Appendix II. The electronic portion of the device was designed by Mr. J. L. Roof, and constructed by Mr. J. L. Roof and the writer. The electronic circuit is capable of measuring illuminations corresponding to phototube currents of 10^{-10} amperes. A bridge arrangement in the circuit makes the zero setting of the device practically independent of line voltage variations. By use of a voltage-regulated screen supply the sensitivity of the circuit is negligibly affected by variations in the line voltage.

A Kodak Step Wedge (uncalibrated) was used to test the accuracy of the measurement of density by the device. The density of the Step Wedge varied from 0.05 to 3.05 (approximately) in eleven steps. A series of readings was made, from which the probable error was calculated at various points of density. In the range from 0.50 to 2.00 the average probable error was 1.0% of the measured density.

The writer measured the density of Weissenberg spots by use of the following experimental arrangement. Light from a 500 watt projection lamp was passed through a water cell, which absorbed the infra-red rays, and then fell on the mirror of a petrographic microscope. The light was reflected up through the Weissenberg spot, which lay between two glass plates on the microscope stage. After passing through the spot, the light entered the objective, and upon emerging from the ocular, entered the photocell connected to the electronic portion of the microphotodensitometer.

By suitable magnification ratios and a metal disk diaphragm placed at the critical focus of the ocular, the density of various areas on the film can be investigated.

Two methods of approach can be followed in the measurement of density. If the Weissenberg spot is assumed to be a cylinder of darkness in the emulsion, then the logarithm of the ratio of the light transmitted through the background of the film to the light transmitted through the center of the Weissenberg spot yields the density of the spot. This density, in turn, can be related to the relative intensity of the X-rays causing the spot. This was done

through the use of the experimental density vs. exposure curve for the level. By use of the proper magnification ratio and the hole diameter in the metal disk diaphragm mentioned above, an extremely small area of the film can be investigated. In this arrangement the Weissenberg spot can be traversed, and the density distribution of the spot in the emulsion can be determined. The integrated intensity of the spot is found by the summation over the points of the spot.

Private communication with Professor W. N. Lipscomb of the University of Minnesota has revealed that the use of a curve of relative "maximum" intensity gives atomic parameters that are negligibly different from those determined from a "density distribution" curve. The short amount of time necessary to determine a "maximum" curve as compared to a "density distribution" curve indicates that the former should be used, especially since both result in the same degree of accuracy in atomic parameters.

X-ray intensity data for ferric acetylacetonate were obtained from Weissenberg photographs about the c axis. The "maximum" density of the Weissenberg spots was measured as outlined above, and converted to relative intensity through the use of the experimental density vs. exposure curves. These values of intensity were corrected by Lorentz factors and polarization factors in the usual way. The structure factors obtained from the corrected relative intensity were placed on the absolute scale by comparison with the calculated values of the structure factors obtained

in the later stages of the analysis. In all, seven levels ($\ell = 6$) or reflections from 9,828 planes were examined. In terms of unitary structure factors, $U = F_{hk\ell}/F_{000}$, two reflections, $\{020\}$ and $\{210\}$, have values of $U = 0.3$, and all others have values of $U < 0.1$.

DETERMINATION OF THE TRIAL STRUCTURE

The trial structure was deduced by use of Harker sections, Patterson projections, and electron density projections. The Harker sections were used to find the position of the Fe atom. Patterson projections were used to determine the orientation of the $Fe-O_6$ octahedron. Electron density projections were used to distinguish between the various ways the carbon atoms can be attached to the $Fe-O_6$ octahedron.

Harker sections are evaluations in Patterson space of particular lines or planes. Harker (1936) showed that for a crystal containing certain symmetry elements, a section along a line or a plane through the three-dimensional Patterson function is related to a projection of the crystal structure on this line or plane. The peaks which occur in this Harker section correspond to vectors between equivalent atoms of the structure. In the space group Pbca a c glide plane of symmetry occurs perpendicular to the b axis. The determination of the Harker section for this symmetry element takes the form of the evaluation of points on the line u = 0, w = c/2, the formula for which is

$$P(0,v,c/2) = \sum\sum\sum \left|F_{hk\ell}\right|^2 \cos 2\pi(kv + \ell/2)$$

$$= \sum_k (B_k)\cos 2\pi kv$$

where

$$B_k = \sum_{h\ell} (-1)^{\ell} \left|F_{hk\ell}\right|^2$$

The information given by this formula is the distance of an atom from the glide plane. This distance is 1/2 the value of v corresponding to a maximum. Similar equations can be derived for the a and b glides of Pbca.

The Harker sections corresponding to the glide planes of Pbca for ferric acetylacetonate are given in Figure 1. The scale is arbitrary and the maximum peaks correspond to Fe-Fe vectors. From these sections the trial coordinates of the Fe atoms were determined to be:

Fe atom: $x = 1/8 \pm \Delta x$ or $3/8 \pm \Delta x$

$y = 1/4$

$z = 1/4$

where $\Delta x = 0.018$

These coordinates are for the octant of the unit cell bounded by planes at x = 1/2, y = 1/2, and z = 1/2. Equivalent coordinates in other octants can be derived by use of the glide planes.

Patterson projections (Patterson 1934) on axial planes contain, superimposed upon one another, all of the interatomic vectors of the unit cell of a crystal. The formula for a Patterson projection on (001) is

$$P(uv) = \sum_{hk\ell} \sum \sum \left| F_{hk0} \right|^2 \cos 2\pi (hu + kv)$$

All the signs of the coefficients are positive since the coefficients are equal to $\left| F_{hk0} \right|^2$. Normally these diagrams are difficult to interpret, particularly with regard to the vectors among the light atoms. However, in

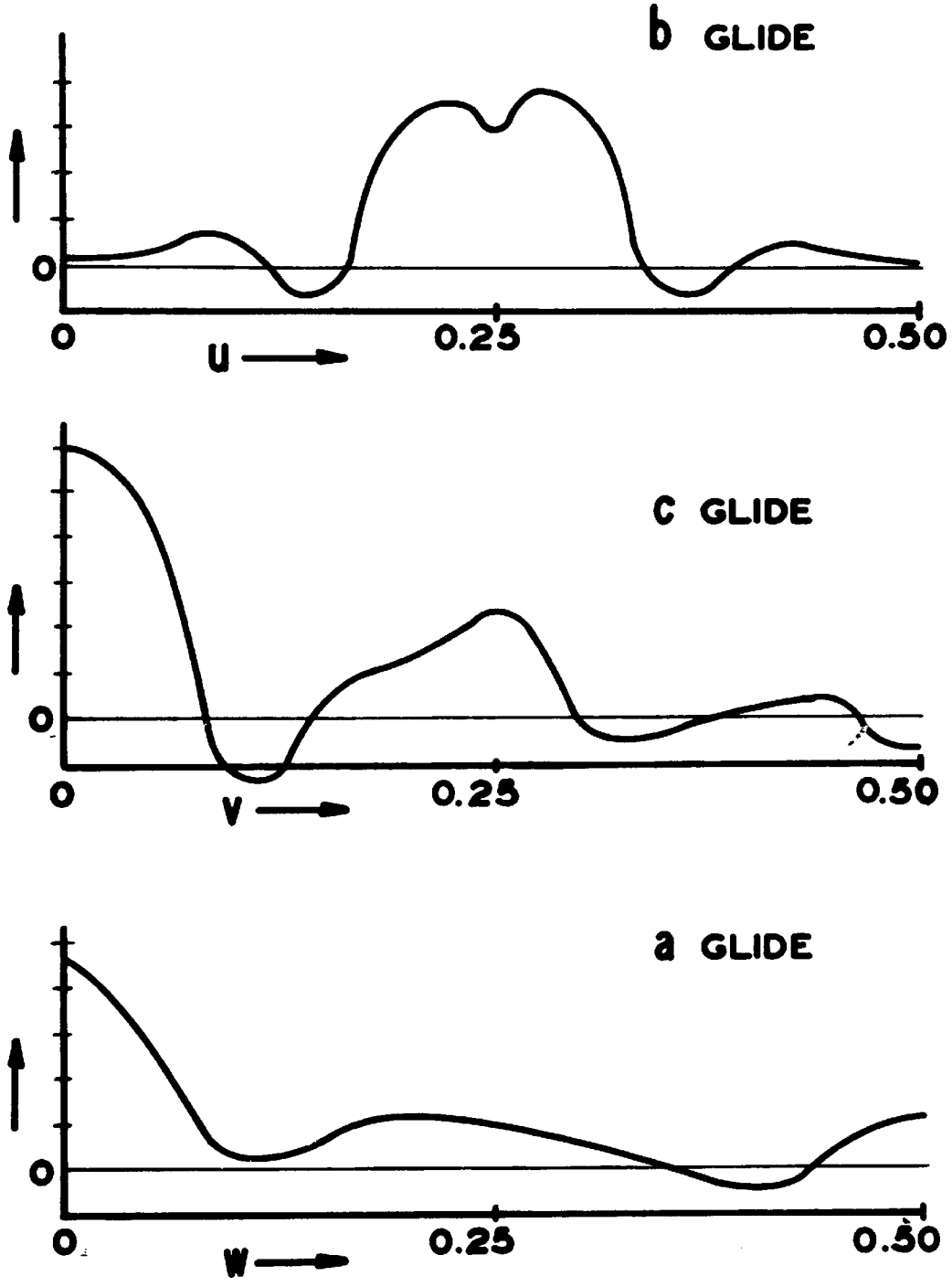


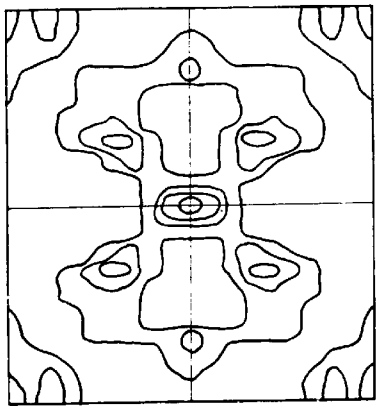
FIGURE 1 HARKER SECTIONS

the case of ferric acetylacetonate the Fe-O distance in the $Fe-O_6$ octahedron lies somewhere between 1.5 and 2.5 Å. Since Fe-O is a moderately strong vector, the examination of the Patterson projection in the region 1.5 to 2.5 Å. from the origin should reveal the Fe-O peaks and thus the orientation of the $Fe-O_6$ octahedron. The Patterson projection on the three axial planes and their interpretation in terms of the $Fe-O_6$ octahedron are shown in Figure 2. Projection on (001) involves two molecules, projection on (010) involves essentially one molecule, and projection on (100) involves two molecules. From these projections the most probable Fe-O distance of 1.96 Å. was deduced.

Electron density projections (Booth, 1948; James, 1948) are more effective techniques for structure analysis than Patterson projections, since they reveal the positions of the atoms in the unit cell instead of only the vector distance between atoms. The electron density of ferric acetylacetonate was projected on the (001) plane, as this projection results in the greatest resolution between the atoms. The formula for the projection of electron density on the (001) plane is

$$\rho_{xy} = \frac{1}{A} \sum_{hk} (F_{hk0}) \cos 2\pi(hx + ky)$$

There is no $\sin 2\pi(hx + ky)$ term as the projection has a center of symmetry. The evaluation of this equation requires the determination of the signs of the coefficients.

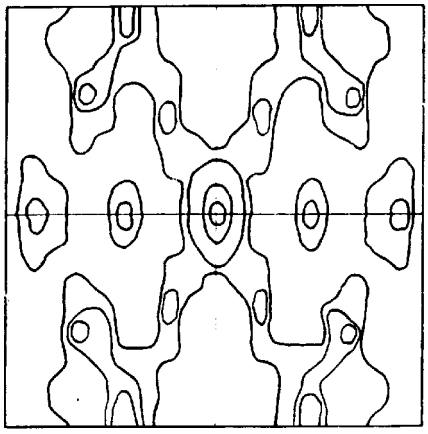


001

0.25 V

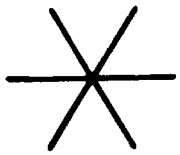


0.25 U

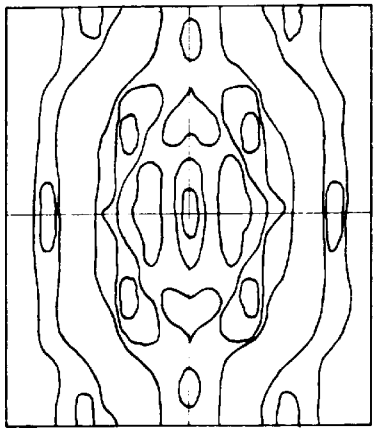


010

0.25 U

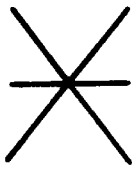


0.25 W



100

0.25 V



0.25 W

FIGURE 2 PATTERSON PROJECTIONS

The signs of the coefficients were determined by the "heavy-atom" method (Booth 1948). This assumes that the sum of the squares of the atomic numbers of the heavy atoms and of the light atoms are approximately equal. For ferric acetylacetonate the atomic number of iron, squared, equals 676. The atomic number of oxygen, squared, equals 64, and the atomic number of carbon, squared, equals 36. For the six oxygen atoms and the fifteen carbon atoms of ferric acetylacetonate the sum of the atomic numbers, squared, equals (6 x 64) + (15 x 36) = 924. If the average contribution of the heavy atoms approximates the average contribution of the light atoms, the signs of about three quarters of the structure factors will be correct. Half will be correct because of the probability that the two contributions have the same sign. Of the remainder, half will be correct because of the probability that the contributions of the light atoms are opposite in sign to, but less than, the contributions of the heavy atoms.

There are several ways in which the carbon atoms may be joined to the $Fe\text{-}O_6$ octahedron. The purpose of the electron density projection on (001) is to distinguish between the various possibilities. For the determination of the signs of the coefficients the Fe atom is placed at $x = 1/8$, $y = 1/4$, $z = 1/4$. If the Fe atom is placed at $x = 1/8 \pm \Delta x$ then, depending on whether Δx is positive or negative, there will be a change in sign of hk0 with h = 2, 6, 10, ... and k = even; and hk0 with h = 4, 8, 12, ... and k = odd. For the trial projection these terms with variable

signs dependent on Δx are eliminated from the series. If the Fe atom is placed at $x = 3/8$, only the hk0 terms with k odd change sign. This amounts to placing the molecule on the opposite side of the b glide plane, but it does not change the way the carbon atoms are attached to the $Fe\text{-}O_6$ octahedron.

The trial projection of electron density on (001), the signs of the series determined by the iron atom, is shown in Figure 3. The contours are at arbitrary intervals. The projection clearly shows the manner in which the carbon atoms are attached to the $Fe\text{-}O_6$ octahedron. Since this is a projection of all the diffracting matter from 0 to c in the unit cell, the projection involves the superposition of two molecules.

Since the projection of electron density on (001) involves two molecules related by a glide plane, there are four ways to interpret Figure 3. Theoretically there are four positions at which to place the iron atom. These four positions differ only in their x coordinates. These four positions, coupled with four ways of interpretation, result in sixteen sets of atomic coordinates. For the hk0 reflections each of the sixteen sets produced calculated structure factors equal in numerical magnitude to each other. However, each of the sixteen sets is related to each other by the symmetry of reflection. The question of which set represents the structure of the crystal is reduced to the arbitrary choice of initial orientation of

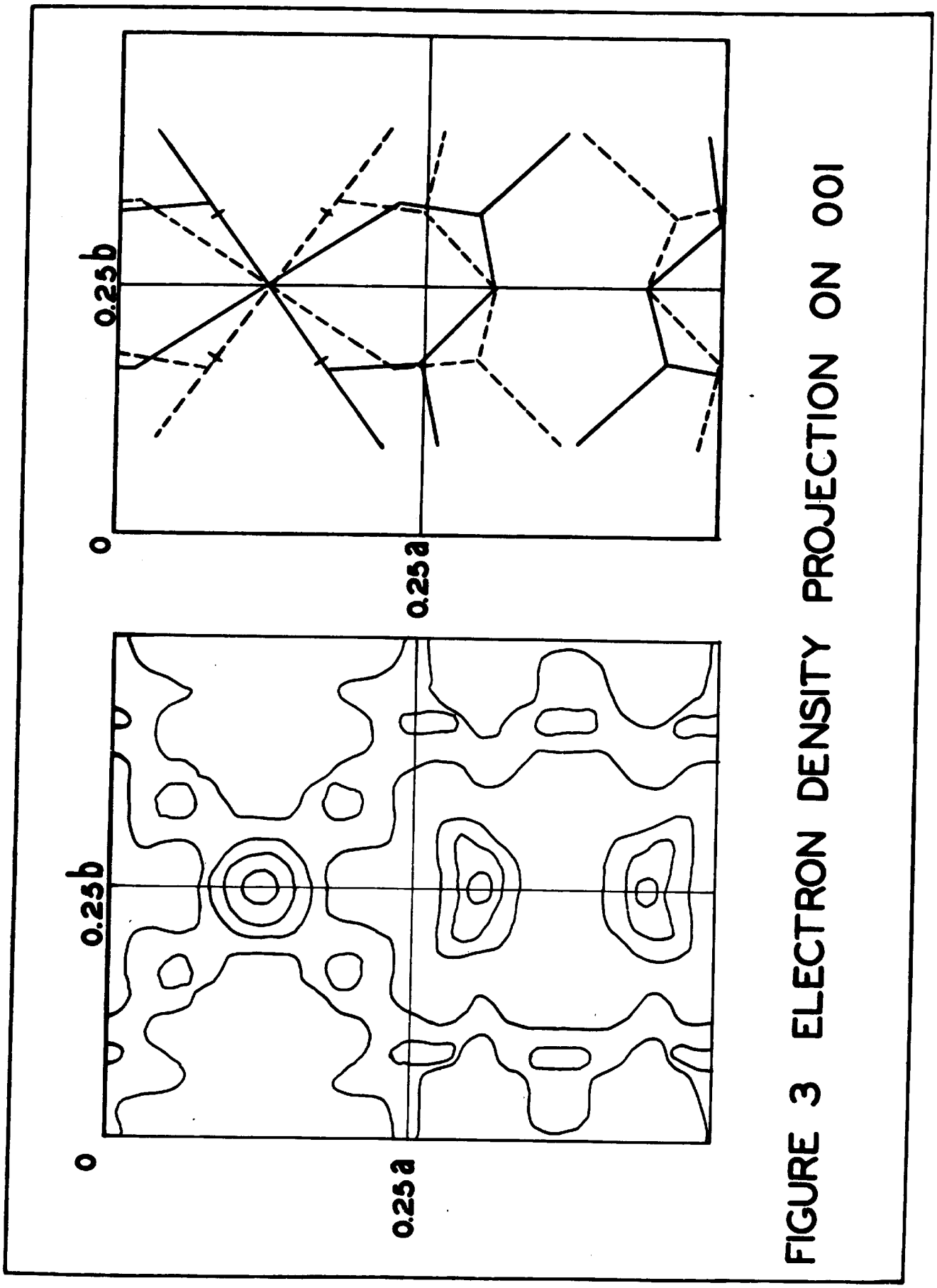


FIGURE 3 ELECTRON DENSITY PROJECTION ON 001

the molecule. Since each of the sixteen sets is equivalent to one another, the arbitrary selection of one set adequately represents the structure of the crystal.

The sixteen sets of equivalent atomic coordinates can be reduced to eight by the consideration of the upper Weissenberg levels involving the z coordinates of the atoms. Calculations for the hkl reflections reveal that each of the four sets of atomic coordinates characterized by Fe = $1/8 + \Delta x$, and each of the four sets of atomic coordinates characterized by Fe = $3/8 - \Delta x$, produce calculated structure factors equal in numerical magnitude to each other. There is good agreement with the observed structure factors as shown in Figure 4. The eight sets, four at Fe = $1/8 - \Delta x$ and four at $3/8 + \Delta x$, also produce calculated structure factors equal in numerical magnitude to each other, but these structure factors do not agree well with the observed reflections as shown in Figure 4. Therefore, these coordinates, $1/8 - \Delta x$ and $3/8 + \Delta x$, need not be considered again.

In the hkl reflections only h odd can produce changes in the numerical magnitude of the structure factors. Since the Fe atom must be located $\pm \Delta x$ of the $x = 1/8$ position, then, for h even, for both sine and cosine waves, there is a symmetry relationship between $\pm \Delta x$ that results either in change of sign or no change of sign, but always no change in numerical magnitude. For h odd this symmetry relationship does not exist, and a change in numerical

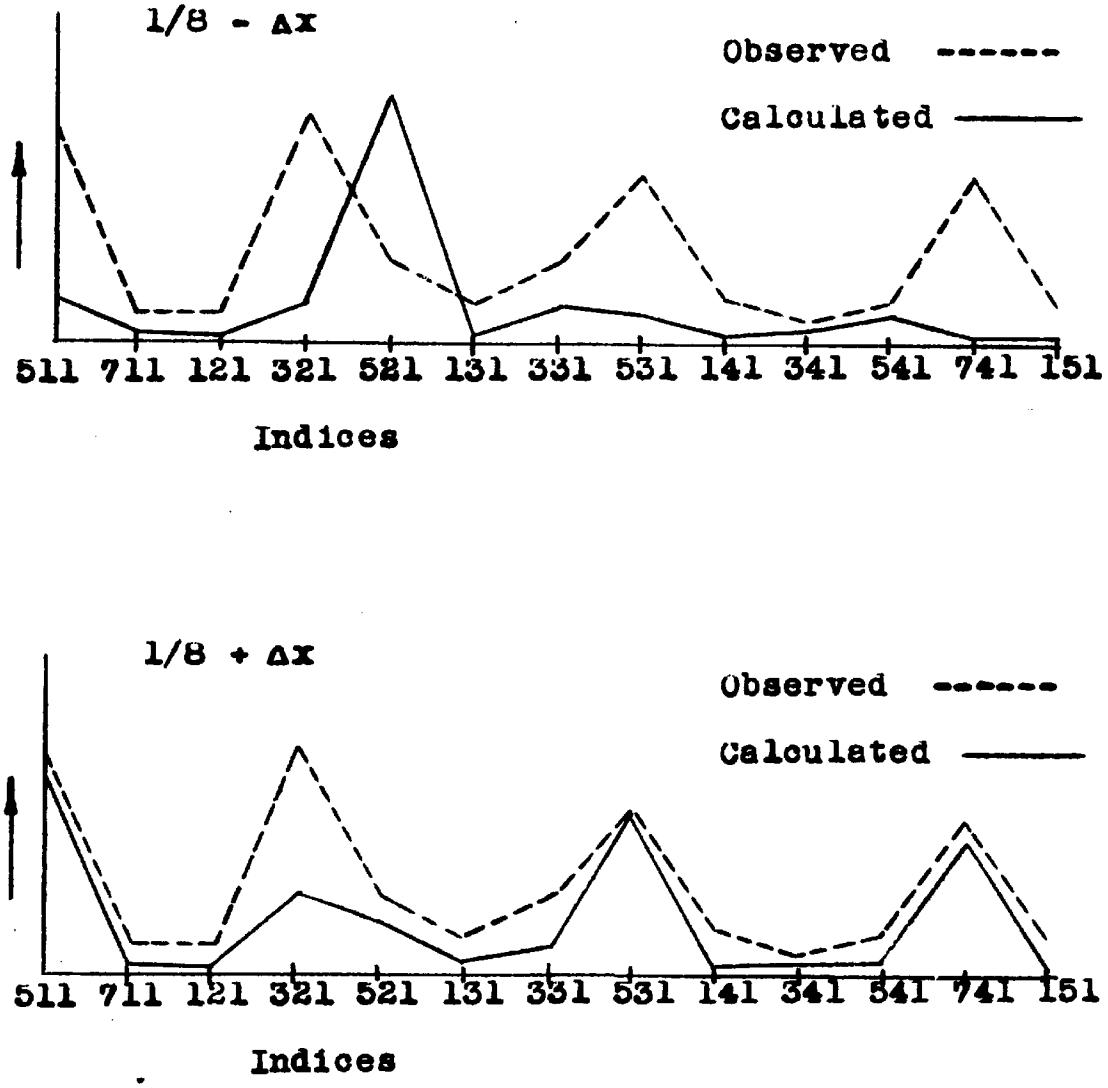


Figure 4. Rerlections for hkl

magnitude can be effected. Therefore, in Figure 4, only hkl with h odd are shown.

In the hkl reflections, as in the hk0 reflections, the eight sets are related to each other by the symmetry of reflection, and the question of which one represents the structure is reduced to the arbitrary choice of initial orientation of the molecule. Since the eight sets are equivalent to each other, the selection of any one will adequately represent the structure of the crystal and allow corrections to interatomic distances to be calculated.

One of the sets of atomic coordinates characterized by $Fe = 1/8 + \Delta x$ was selected as the basis from which refinements to the atomic parameters were calculated.

REFINEMENT OF ATOMIC COORDINATES

Since the electron density projection on (001) contains the superposition of two molecules, there is overlapping of various interatomic distances and atomic coordinates cannot be accurately assigned. For the refinement of the atomic coordinates the electron density corresponding to only one molecule was projected on (001). This was done through the use of a partial three-dimensional Fourier summation termed the bounded projection. As this is not a standardized formula its derivation and application to ferric acetylacetonate is given below.

The most popular method of application of Fourier Series has proved to be the two-dimensional projection. The work involved in obtaining the data for and summing a three dimensional series is so great that, in general, it is reserved for the most important problems. Several compromises may, however, be arrived at; information may be obtained from a knowledge of the data contained in the complete observable reciprocal lattice without the necessity for the complete summation of the three-dimensional series. One of these compromises is the projection of the contents of the unit cell lying between two planes, for instance, $z = z_1$ and $z = z_2$ (the bounded projection). If interest lies in the $\underline{x}$ and $\underline{y}$ parameters of atoms that are known to lie between these two planes, there is no need to consider the $\underline{z}$ coordinates of the atoms.

Let the density projected in this way be $\rho_{12}(xy)$. Then

$$\rho_{12}(xy) = \int_{z_1}^{z_2} \rho(x,y,z)\, c\, dz$$

Substituting

$$\rho(x,y,z) = \frac{1}{V}\Sigma\Sigma\Sigma F(hk\ell)\, \exp\{-2\pi i(hx + ky + \ell z)\}$$

for the electron density

$$\rho_{12}(xy) = \frac{c}{V}\int_{z_1}^{z_2}\Sigma\Sigma\Sigma F(hk\ell)\left[\exp\{-2\pi i(hx + ky + \ell z)\}\right] dz$$

is obtained.

Integration yields

$$\rho_{12}(xy) = \frac{1}{A_c}\Sigma\Sigma\Sigma \frac{F(hk\ell)}{-2\pi i\ell}\left[\exp\{-2\pi i(hx + ky + \ell z_2)\} - \exp\{-2\pi i(hx + ky + \ell z_1)\}\right]$$

Expansion yields

$$\rho_{12}(xy) = \frac{1}{A_c}\Sigma\Sigma\Sigma \frac{F(hk\ell)}{2\pi\ell}\left[\sin 2\pi(hx + ky + \ell z_2) + i\cos 2\pi(hx + ky + \ell z_2) - \sin 2\pi(hx + ky + \ell z_1) - i\cos 2\pi(hx + ky + \ell z_1)\right]$$

Trigonometric identities yield

$$\rho_{12}(xy) = \frac{1}{A_c}\Sigma\Sigma\Sigma \frac{F(hk\ell)}{2\pi\ell}\left[2\cos 2\pi\left(hx+ky+\ell\frac{(z_2+z_1)}{2}\right)\sin 2\pi\ell\frac{(z_2-z_1)}{2} - 2i\sin 2\pi\left(hx+ky+\ell\frac{(z_2+z_1)}{2}\right)\sin 2\pi\ell\frac{(z_2-z_1)}{2}\right]$$

which can be written as

$$\rho_{12}(xy) = \frac{1}{A_c}\sum\sum\sum \frac{F(hk\ell)}{\pi\ell} \sin 2\pi\ell\left(\frac{z_2-z_1}{2}\right)\left\{\exp -2\pi i\left(hx+ky+\ell\left(\frac{z_2+z_1}{2}\right)\right)\right\}$$

Elimination of complex quantities yields

$$\rho_{12}(xy) = \frac{1}{A_c}\sum\sum\sum \frac{F(hk\ell)}{\pi\ell} \sin 2\pi\ell\left(\frac{z_2-z_1}{2}\right)\left\{\cos 2\pi\left(hx+ky+\ell\left(\frac{z_2+z_1}{2}\right) - a_{hk\ell}\right)\right\}$$

the summation taken over half of the reciprocal lattice. For a crystal with a center of symmetry the phase angle $a_{hk\ell}$ reduces to the indetermination of the sign + or - for the structure factor and the summation may be expressed as

$$\rho_{12}(xy) = \frac{1}{A_c}\sum\sum\sum\left[F(hk\ell)\ \frac{\sin 2\pi\ell\left(\frac{z_2-z_1}{2}\right)\cos 2\pi\ell\left(\frac{z_2+z_1}{2}\right)\cos\ 2\pi(hx+ky)}{\pi\ell}\right.$$

$$\left. -F(hk\ell)\ \frac{\sin 2\pi\ell\left(\frac{z_2-z_1}{2}\right)\sin 2\pi\ell\left(\frac{z_2+z_1}{2}\right)\sin\ 2\pi(hx+ky)}{\pi\ell}\right]$$

Thus the quantities $F(hk\ell)$ have to be multiplied by factors which, for given values of z_2 and z_1 are functions of ℓ only, and they can therefore be evaluated separately for the few different values of ℓ to be considered. After the new coefficients have been obtained, the summation follows the ordinary lines of a two-dimensional summation.

While the computational work is still as large as for a two-dimensional analysis, it is also necessary that all of the values of $F(hk\ell)$ be known, and thus the interpretation of photographs and the derivation of structure factors is still as difficult as for a complete three-dimensional

analysis. In special cases this work can be reduced to some extent. For example, if the contents of half the unit cell are projected, $z_2-z_1 = 1/2$, and thus the value of $\sin 2\pi l\left(\frac{z_2-z_1}{2}\right)$ is zero if l is even; consequently, the reflections with l even, but not zero, need not be measured. If l is zero, the quantity $\sin 2\pi l(z_2-z_1)/2\pi l$ is equal to z_2-z_1 (limit of $\sin 2\pi l/2\pi l$ as $2\pi l$ approaches zero equals one) and so the terms with l zero do not disappear when a bounded projection is determined.

The above formula was applied to ferric acetylacetonate in the following manner. Since only one molecule, which is contained in the lower half or the unit cell was projected, the boundaries were $z_2 = 1/2$ and $z_1 = 0$. For these boundary limits the factors dependent on l by which the coefficients or the series are multiplied were calculated

0-level -- 1/2

1-level -- $1/\pi \sim 1/3$

2-level -- $1/3\pi \sim 1/10$

3-level -- $1/5\pi \sim 1/16$

Only the zero and the first level were used in the bounded projection (775 terms in the series). The third and fifth levels have coefficients that are small initially, and when multiplied by factors of 1/10 and 1/16 the coefficients are reduced to negligible quantities.

The signs of the coefficients were determined from the calculated structure factors. Initially, one of the

eight equivalent sets or atomic coordinates was chosen and structure factors were calculated for this set. Atomic scattering factors were taken from the International Tables with the iron factor corrected for dispersion of the electrons in the K shell, since iron radiation was used. Summations were made on Dr. H. J. Grenville-Wells' Moving-Strip Fourier Analyzer, which is an adaptation of Robertson's sorting board (Robertson 1936). All summations were performed on desk calculating machines. After each summation, changes in atomic parameters were noted and a new set of signs was calculated for the next summation. The coefficients themselves were the observed structure factors.

After nine summations of the series, the iron atom, the oxygen atoms, and thirteen of the fifteen carbon atoms were resolved. From the electron density map, Figure 5 was prepared. Crosses represent the electron density peaks, and a line diagram of the molecule is shown.

The agreement between the predicted and observed points or maxima is excellent, considering that two important correction factors have not been applied; namely, temperature effects and the contributions of the hydrogen atoms.

The implied correction shown in the diagram, i.e., the movement of the Fe atom to coincide with the observed electron density peak was believed not to be valid in view of the resolution obtained for the other atoms. This proved to be correct, as in a new summation with this correction applied, enough signs of the coefficients were changed so that the resolution obtained was inferior to that shown in

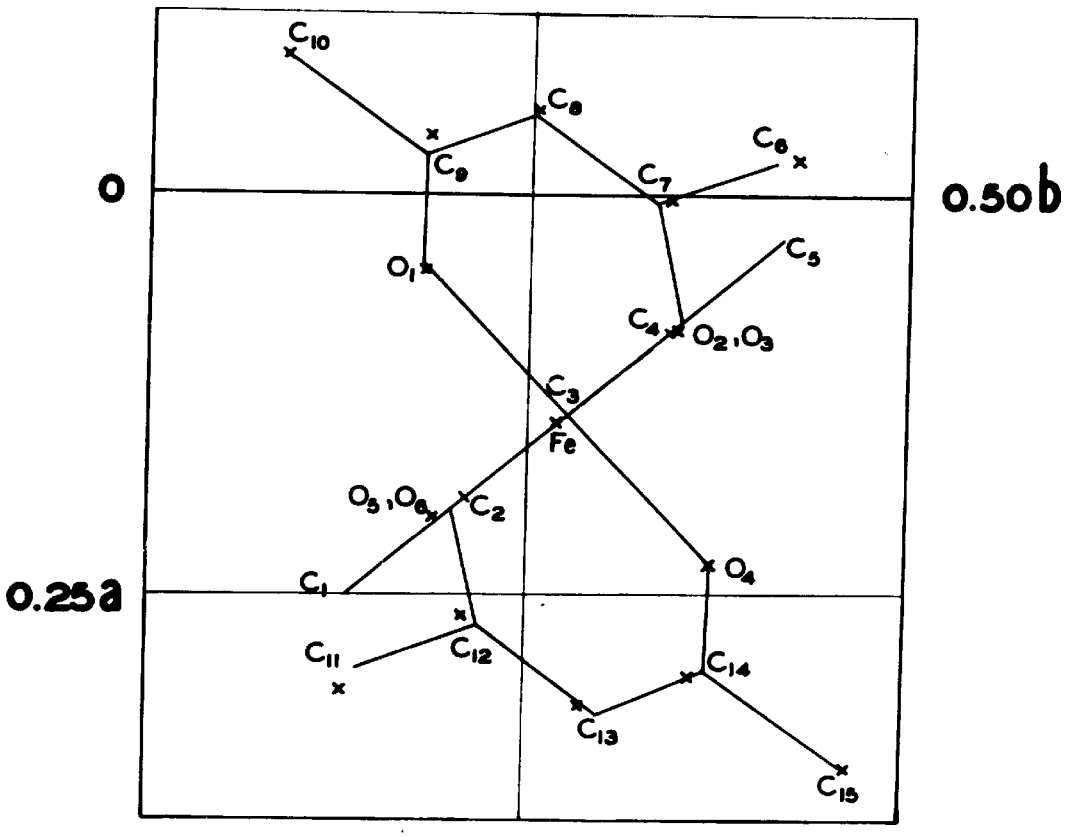


FIGURE 5 FINAL ORIENTATION OF THE MOLECULE

Figure 5. Thus the final atomic coordinates x and y are those shown in Figure 5. The final z coordinates were calculated from measurements on this projection.

LOCATION OF HYDROGEN ATOMS

In an attempt to locate the hydrogen atoms of the ferric acetylacetonate molecule, a difference projection was computed using $F(hk\ell)_o - F(hk\ell)_c$ as coefficients of the series. The relationship between $F(hk\ell)_o$ and $F(hk\ell)_c$ is given by the following formula

$$k\,F(hk\ell)_o = F(hk\ell)_c\, e^{-B\frac{\sin^2\theta}{\lambda^2}}$$

where

k = scale factor placing the observed structure factors on the absolute scale

$F(hk\ell)_o$ = observed structure factor

$F(hk\ell)_c$ = calculated " "

$e^{-B\frac{\sin^2\theta}{\lambda^2}}$ = normal isotropic temperature factor, where B is an experimental constant

The average ratio of F_c/F_o for several ranges or $\sin^2\theta/\lambda^2$ was plotted on semi-log paper, and the best straight line was drawn through the points. The intercept is equal to k and the slope of the line equals $B/2.303$.

The difference projection could not be interpreted in terms of hydrogen atoms. Not only were the hydrogen atoms not resolved, but the areas of positive electron density where hydrogen atoms should appear were absent. The only conclusion is that hydrogen atoms contribute little or nothing to the structure factors of ferric acetylacetonate.

Therefore, theoretical coordinates were assigned to the hydrogen atoms with the carbon-hydrogen distance assumed to be 1.09 Å. The principle of the most efficient utilization of available space was used to orient the hydrogen atoms in the methyl groups.

EVALUATION OF THE RESIDUAL

It has been found useful to express the overall agreement of structure factors in terms of the mean discrepancy, or the residual,

$$R = \frac{\Sigma\left(|F_o| - |F_c|\right)}{\Sigma|F_o|}$$

where $|F_o|$ and $|F_c|$ are the moduli of the observed and calculated structure factors, and the summation is taken over all the reflections.

Values of R can be a useful guide in deciding whether any particular change in parameters has produced any improvement in the agreement. There is also a tendency in current crystallographic research to use the residual as a quantity for comparison of the accuracy of the determination of different crystal structures. This procedure is not recommended. A complicated crystal structure may give a large number of very weak reflections, for which the average discrepancy will be quite large; and thus the residual will be rather large compared with that given by a much simpler structure, but the correctness is not thereby disproved. Care must be taken not to place too much weight on the actual value of the residual; there is no particular value that must be reached before a structure becomes acceptable, nor does the attainment of a particular value necessarily prove that the structure is correct. The most reliable procedure at the present time seems to be the

solution or electron density projections coupled with the use of the residual as a general guide.

Table 2 summarizes the conditions on which the various residuals or ferric acetylacetonate are based, and also the value or the respective residual.

Based on the final positions of the iron, oxygen, and carbon atoms as shown in Figure 5, and the isotropic temperature factor involved, a residual or 0.352 for the zero level and 0.406 for the first level was determined. With the carbon-hydrogen distance of 1.09 Å., and the hydrogen atoms placed in their most probable positions, the value or the residual is 0.363 for the zero level and 0.394 for the first level. This verifies the conclusion made in the prior section that the hydrogen atoms contribute little or nothing to the structure factors of ferric acetylacetonate.

Examination of the individual experimental ratios F_c/F_o reveal that the values fall into three general classes. The large majority show a gradual increase in value with increasing $\sin^2\theta$, which results in the normal temperature factor determination. The remaining minority have either exceptionally large or exceptionally small values.

With negligible absorption assumed, and the effects of hydrogen atoms and temperature accounted for, the discrepancy in the individual experimental ratios implies the operation of double reflections. X-rays which have been reflected from one set of planes may be reflected

TABLE 2

Conditions for Evaluation or Residual

Conditions	0-level	1st-level
Iron, oxygen, carbon isotropic B	0.352	0.406
Iron, oxygen, carbon hydrogen isotropic B	0.363	0.394
Iron, oxygen, carbon hydrogen isotropic B "coupled" double reflections	0.259	0.229
Iron, oxygen, carbon hydrogen anisotropic B "coupled" double reflections	0.185	0.196
Iron, oxygen, carbon hydrogen anisotropic B single reflections	0.169	0.228

from another set of lattice planes which happen, by chance, to be in the correct orientation. These are the "double" reflections of Renninger (1937). Lipson & Cochran (1953) point out that with a complicated crystal this effect must occur quite frequently, but in general, double reflections are extremely weak and so their effects are usually neglected. However, in the case of ferric acetylacetonate, all but two reflections have unitary structure factors of $U < 0.1$ and the effect of double reflections should not be ignored.

The way that double reflections arise may be seen by considering the conditions for reflection as expressed by the sphere of reflection. Figure 6 illustrates the general geometrical conditions. If AO is the direction of the incident beam, the reflection B' in the direction CB' will be produced when the sphere of reflection, whose section in the diagram is AB'O, passes through the reciprocal-lattice point B'. To find the condition under which the reflected beam CB' should be reflected from another set of planes, another sphere of reflection is constructed with the direction CB' as diameter; then if this sphere passes through a reciprocal lattice point, for instance F, then the beam CB' will be reflected to produce an emergent ray C'F. However, the second sphere may be transposed to superimpose on the first sphere, and then the point F is identical with F'. Thus an alternative definition would be that when two or more reciprocal

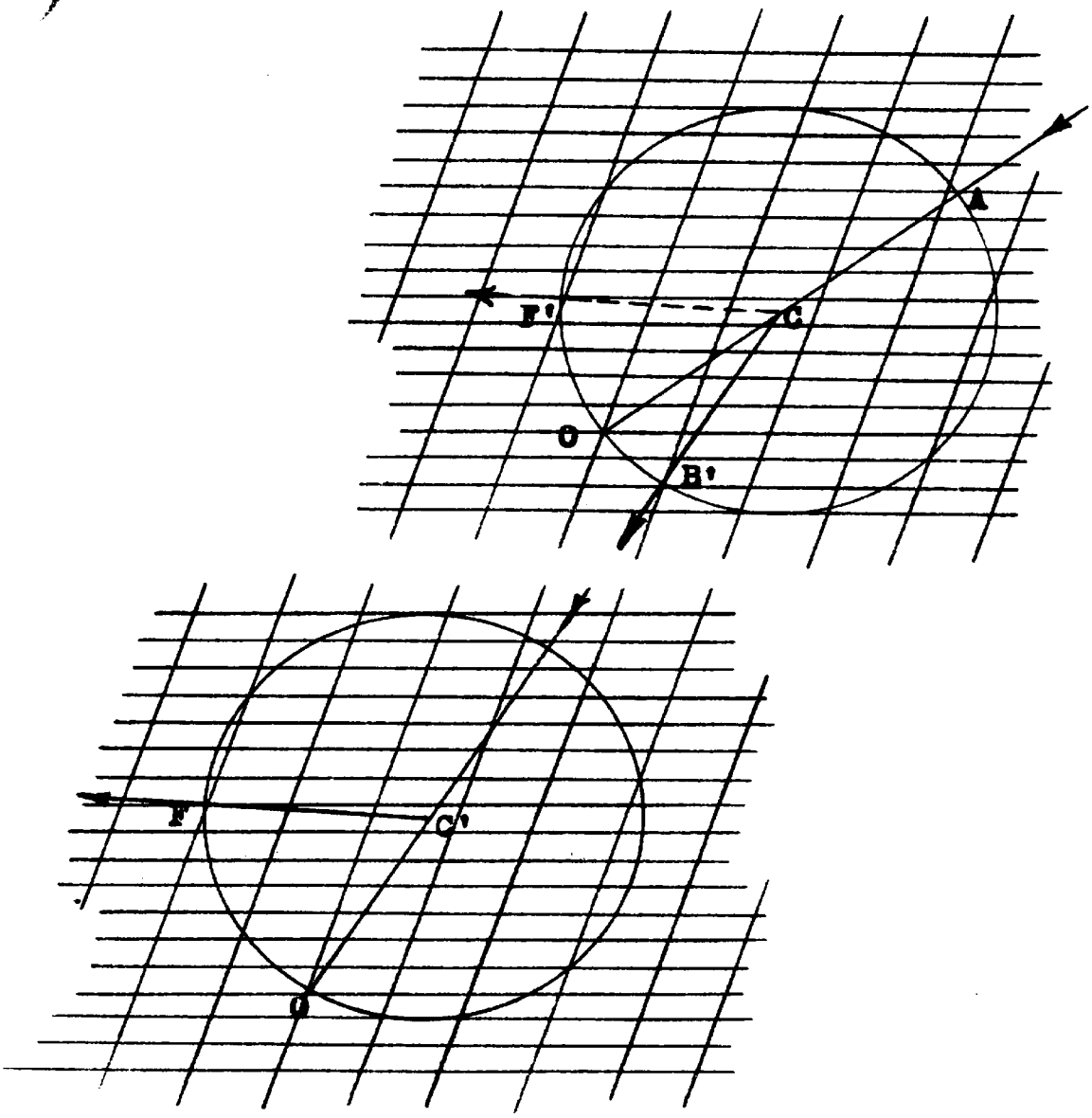


Figure 6. General Geometrical Conditions for "Double" Reflection of X-rays

lattice points pass through the sphere of reflection at the same time "double" reflections may occur.

If the beam CB' is reflected to produce beam CF', then the true value of reflection B' has been decreased and the true value of reflection F' has been increased. Of course this may also occur in the reverse fashion, and thus when there are "double" reflections, each part of the double reflection distorts the true value of the individual reflection in an additive or subtractive manner. The writer suggests that a more nearly correct way to evaluate the diffracting power of the structure in these cases of "double" reflections is to compare the sum of the observed "double" reflection structure factors with the sum of the calculated "double" reflection structure factors. When this is done for ferric acetylacetonate, the value of the residual decreases to 0.259 for the zero level and to 0.229 for the first level. Thus, a significant improvement has been effected by the identification of "double" reflections.

The last experimental factor investigated was an anisotropic temperature factor. An isotropic factor was assumed for convenience in the early calculations. This was based on the fact that the orthorhombic unit cell approximates a cubic cell in dimensions. The value of B in an anisotropic temperature factor will be the largest in the direction in the unit cell in which the molecule can vibrate most freely. For the hk0 reflections

the largest volumes of free space are in the a and b directions and the smallest in the [110] direction. The graph of log F_c/F_o against $\sin^2\theta/\lambda^2$ for h00 and 0k0 results in a value for B of 6.0 while for hk0 with h = k the value for B is zero. These results are shown in Figure 7. The graph of log F_c/F_o for other zones result in intermediate values for B. The variation of B with angle from either the a or b axis is shown in Figure 8.

When the empirically derived anisotropic temperature factor is applied to the calculations, the value of the residual drops to 0.185 for the zero level and 0.196 for the first level. Thus a small improvement is effected by the use of an anisotropic temperature factor in place of an isotropic temperature factor.

If the residual is evaluated for only the single reflections, it is noted that there is no significant improvement in the residual as compared to the case when "double" reflections were included in the evaluation of the residual.

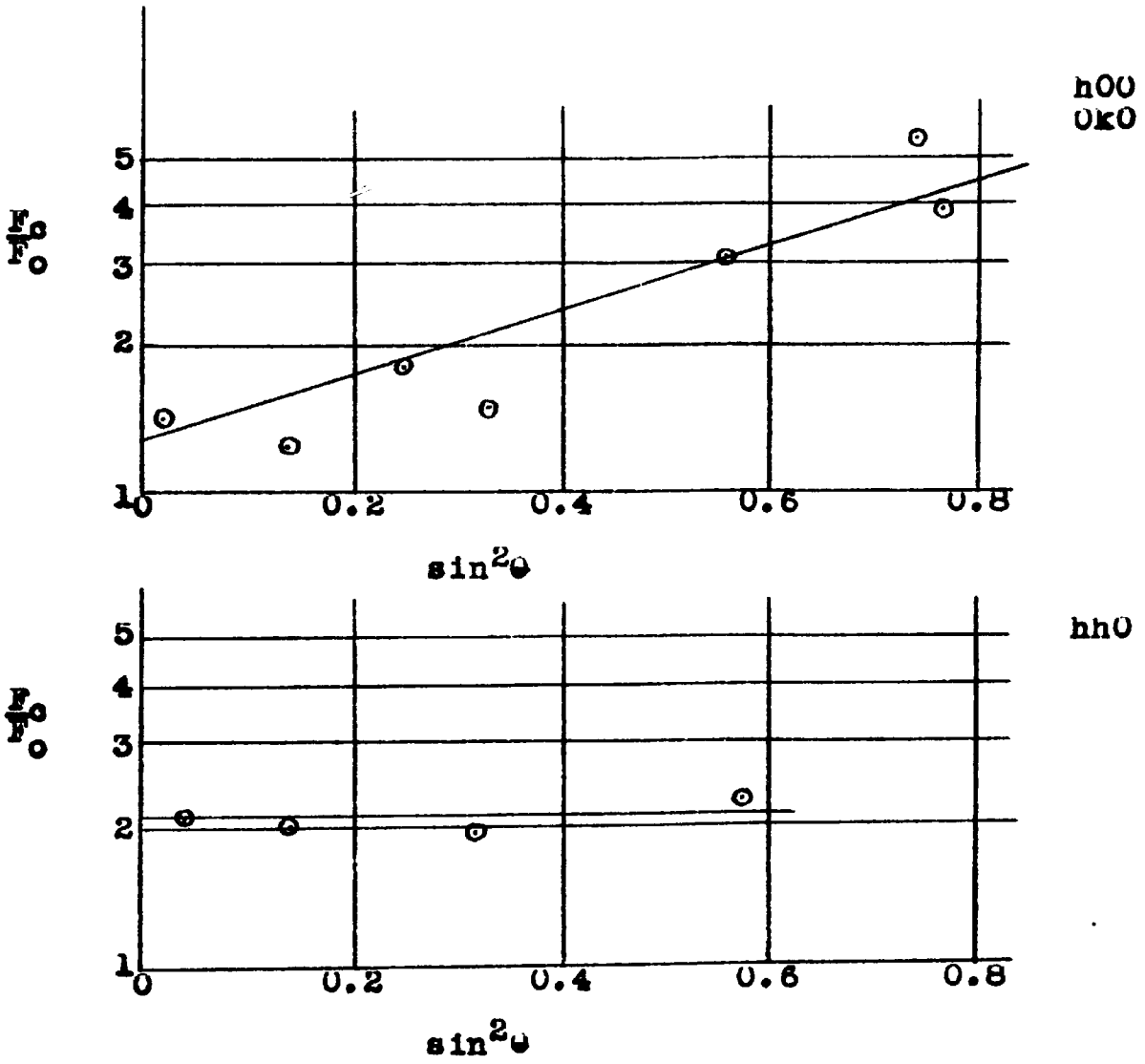


Figure 7. F_c/F_o vs. $\sin^2\theta$

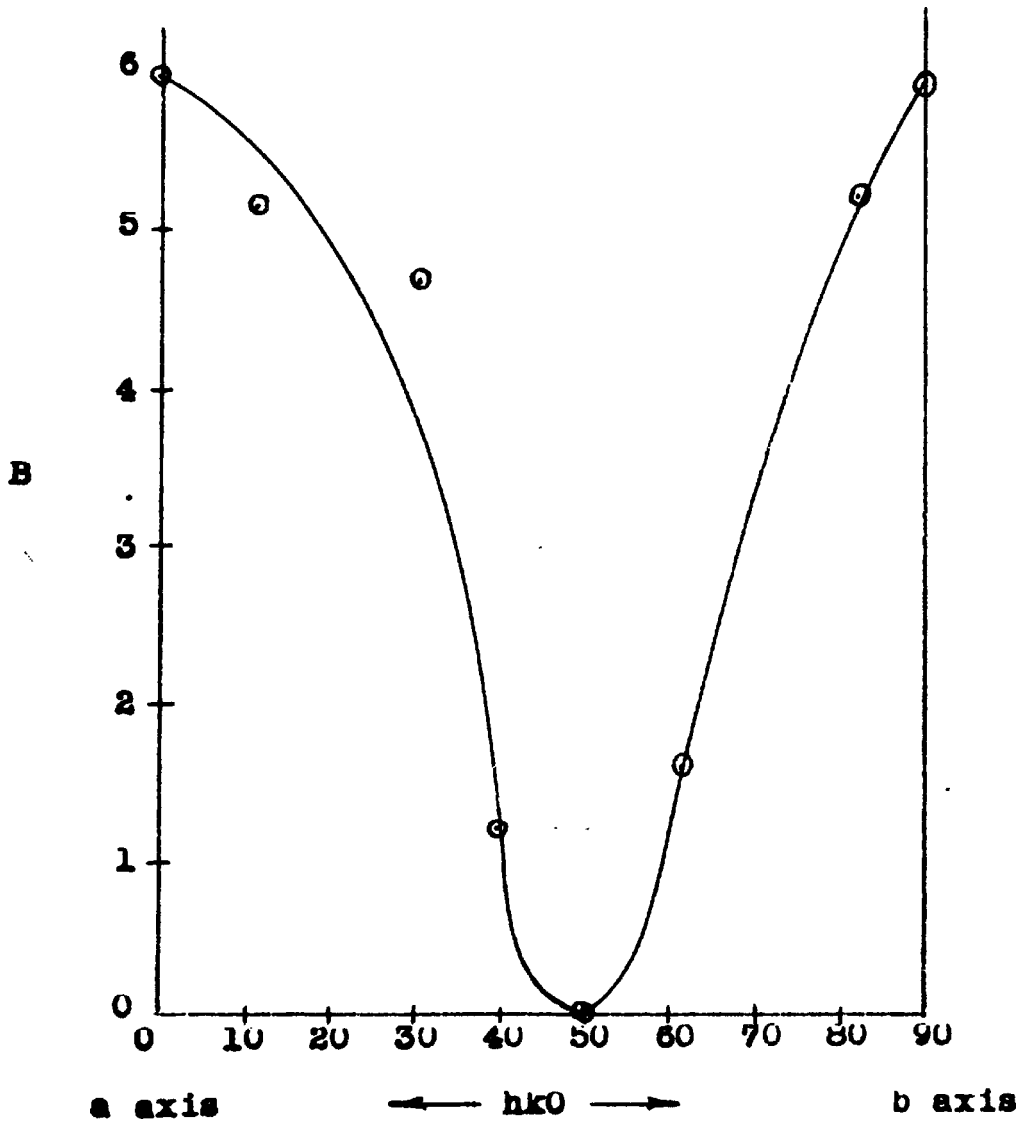


Figure 8. Variation of B with Angle

THE ACCURACY OF THE DETERMINATION

An assessment of the accuracy was made by applying the treatment described by Cruickshank (1949). The standard deviation of the atomic coordinates is given by

$$\sigma(\underline{x}) = \frac{2\pi\left(\Sigma h^2(F_o-F_c)^2\right)^{1/2}}{a\ V\ C_{(x)}}$$

where $\sigma(\underline{x})$ is the standard deviation in the $\underline{x}$ coordinates, "a" is the unit cell edge, V is the volume of the unit cell, and $C_{(x)}$ is the central curvature of the $\underline{n}$th atom in the $\underline{x}$ direction. Similar equations are used for the $\underline{y}$ and $\underline{z}$ coordinates. Since the original equations require that all of the available points of the reciprocal lattice be summed, the above equation, applied to ferric acetylacetonate, was modified by a factor which represented the percentage of theoretical points actually used in the determination.

Costain (1941) first pointed out that the electron density at a distance not far from the center of an atom can be closely approximated by the relation

$$\rho = Z\left(\frac{p}{\pi}\right)^{3/2} \exp(-pr^2)$$

where ρ is the density at a distance "r" from the center of the atom, Z is the atomic number, and "p" is a constant, expressed in Å.^{-2}, which in this case is best obtained from measurements on the electron density map. These measurements are used to give a graph of $\log \rho$ against r^2. The relation requires that

the density be in electrons per cubic Å., $e\text{Å}.^{-3}$ Only the bounded projected electron density, $e\text{Å}.^{-2}$, is available, but since all the atoms are resolved in the bounded projection, then if the projected density is divided by the average diameter of the atom a close approach to $e\text{Å}.^{-3}$ will be obtained. A better approximation would be to multiply the projected density by the ratio of a circle to a sphere.

The graph of log density (corrected bounded projected electron density) against r^2 is shown in Figure 9. From this graph the value of "p" was determined to be: for iron, 3.76, for oxygen, 3.41, and for carbon 3.74.

The central curvature of an atom is the second differential of the relation given by Costain. This is

$$\left(\frac{d^2\rho}{d\,r^2}\right)_{(n)} = -2\,p\,Z_n\,\frac{(p)}{\pi}^{3/2}$$

and when coupled with the values of "p", the values of the central curvature for the various atoms are

for Iron $\left(\frac{d^2\rho}{d\,r^2}\right) = -256\ e\text{Å}.^{-5}$

Oxygen $= -62$

Carbon $= -58$

from which it can be seen that the heaviest atoms of a structure are the ones most accurately determined.

The Gaussian probable errors in the interatomic distances, determined from Cruickshank standard deviations,

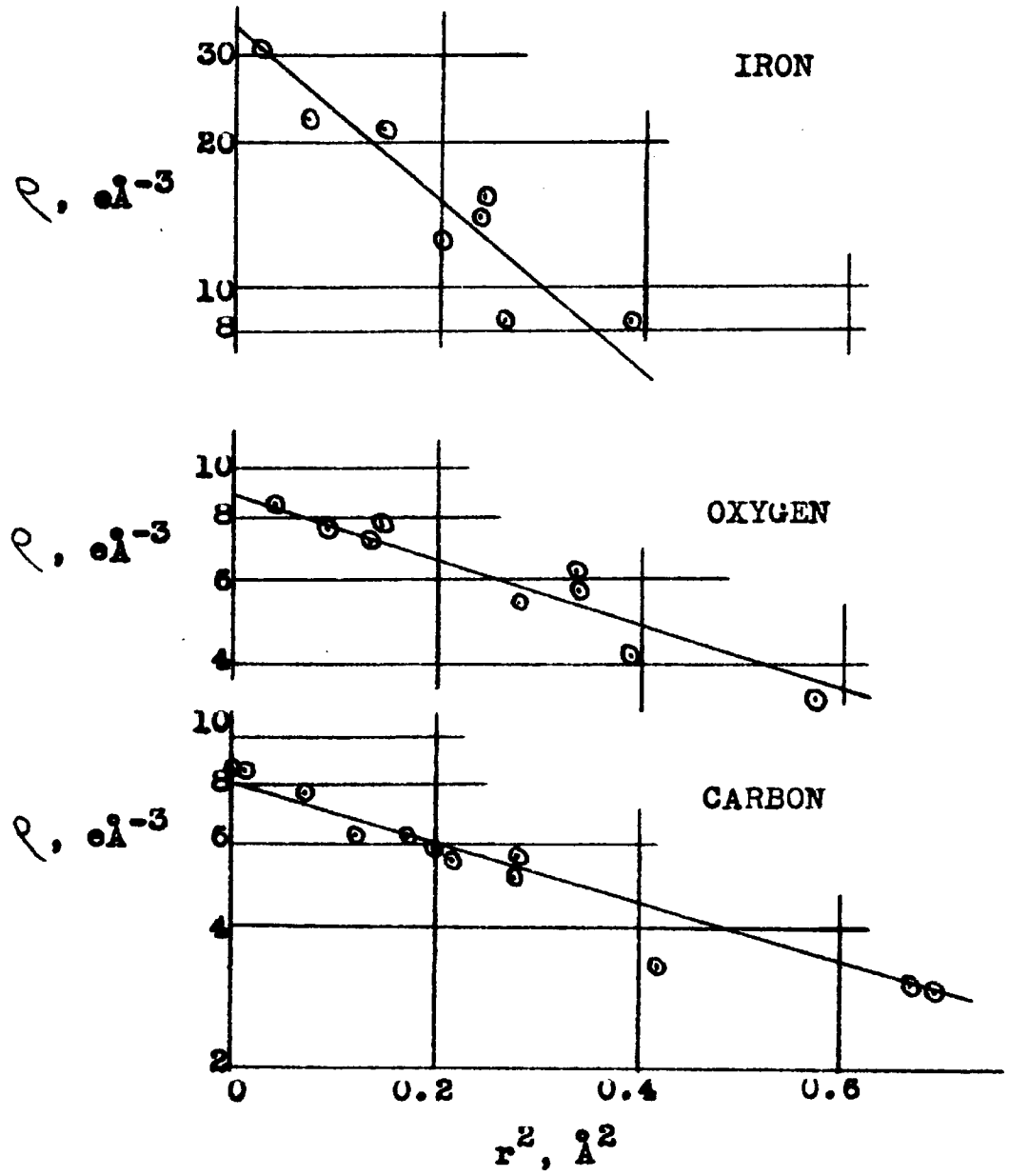


Figure 9. Electron Density vs. r^2

are

Iron-Oxygen	1.96 ± 0.016 Å.
Oxygen-Carbon	1.27 ± 0.022
Carbon-Carbon	1.39 ± 0.023
Carbon-Carbon	1.54 ± 0.023

The limits of error given above are in general agreement with those prevailing in the literature (Lipson & Cochran, 1953); namely, ± 0.02 Å.

In utilizing Cruickshank's formulas, all structure factors with an observed value of zero were assigned values equal to one-half of the minimum value that it was possible to measure with the microphotodensitometer. This procedure was suggested by Smare (1948).

DESCRIPTION OF THE STRUCTURE

The final atomic coordinates of the iron, oxygen, and carbon atoms are given in Table 3. The calculated coordinates of the hydrogen atoms are given in Table 4.

The crystal structure of ferric acetylacetonate consists of discrete molecules linked together in layers by weak Van der Waals forces. The whole unit cell contains eight molecules related by the space group symmetry Pbca. The bond lengths and interbond angles derived from the final atomic coordinates are shown, for one acetylacetonate radical attached to iron, in Figure 10. The light atom interatomic distances are of the proper order of magnitude for normal bond and bond-and-a-half resonance. Thus the assumed octahedral character of the iron is confirmed, as is the dynamic coordination complex model proposed by Morgan (1926). The Iron-Oxygen distance of 1.96 Å. is approximately one-half of the way between a pure ionic bond (2.05 Å.) and a pure covalent bond (1.90 Å.).

The crystal structure projected on (001) is shown in Figure 11. The positions of four molecules, determined by c glide planes perpendicular to the plane of the paper, are not shown in order to avoid confusion. The crystal structure projected on (010) is shown in Figure 12. The positions of four molecules, determined by b glide planes perpendicular to the plane of the paper, are not shown in order to avoid confusion.

TABLE 3

Final Atomic Coordinates for One Molecule
(Seven others related by Pbca)

Atom	x	y	z
Fe	0.136	0.277	0.250
O_1	0.039	0.182	0.250
O_2	0.078	0.352	0.334
O_3	0.078	0.352	0.166
O_4	0.228	0.372	0.250
O_5	0.195	0.200	0.334
O_6	0.195	0.200	0.166
C_1	0.244	0.132	0.051
C_2	0.186	0.211	0.091
C_3	0.136	0.277	0.051
C_4	0.083	0.344	0.091
C_5	0.028	0.420	0.051
C_6	0.997	0.414	0.427
C_7	0.003	0.336	0.366
C_8	0.947	0.254	0.350
C_9	0.972	0.183	0.293
C_{10}	0.911	0.095	0.274
C_{11}	0.292	0.139	0.427
C_{12}	0.266	0.220	0.366
C_{13}	0.322	0.299	0.350
C_{14}	0.297	0.369	0.293
C_{15}	0.354	0.468	0.274

TABLE 4

Coordinates of Hydrogen Atoms (Calculated)

Atom	x	y	z
H_1 (attached to C_1)	0.284	0.092	0.090
H_2 (attached to C_1)	0.216	0.086	0.009
H_3 (attached to C_1)	0.296	0.175	0.009
H_4 (attached to C_3)	0.136	0.277	0.982
H_5 (attached to C_5)	0.068	0.464	0.009
H_6 (attached to C_5)	0.981	0.375	0.009
H_7 (attached to C_5)	0.994	0.458	0.090
H_8 (attached to C_{10})	0.947	0.114	0.257
H_9 (attached to C_{10})	0.914	0.047	0.332
H_{10} (attached to C_{10})	0.852	0.114	0.257
H_{11} (attached to C_8)	0.889	0.242	0.385
H_{12} (attached to C_6)	0.971	0.375	0.490
H_{13} (attached to C_6)	0.916	0.444	0.418
H_{14} (attached to C_6)	0.031	0.465	0.431
H_{15} (attached to C_{15})	0.329	0.508	0.231
H_{16} (attached to C_{15})	0.364	0.505	0.332
H_{17} (attached to C_{15})	0.416	0.439	0.257
H_{18} (attached to C_{13})	0.383	0.311	0.385
H_{19} (attached to C_{11})	0.303	0.175	0.490
H_{20} (attached to C_{11})	0.355	0.108	0.418
H_{21} (attached to C_{11})	0.242	0.086	0.431

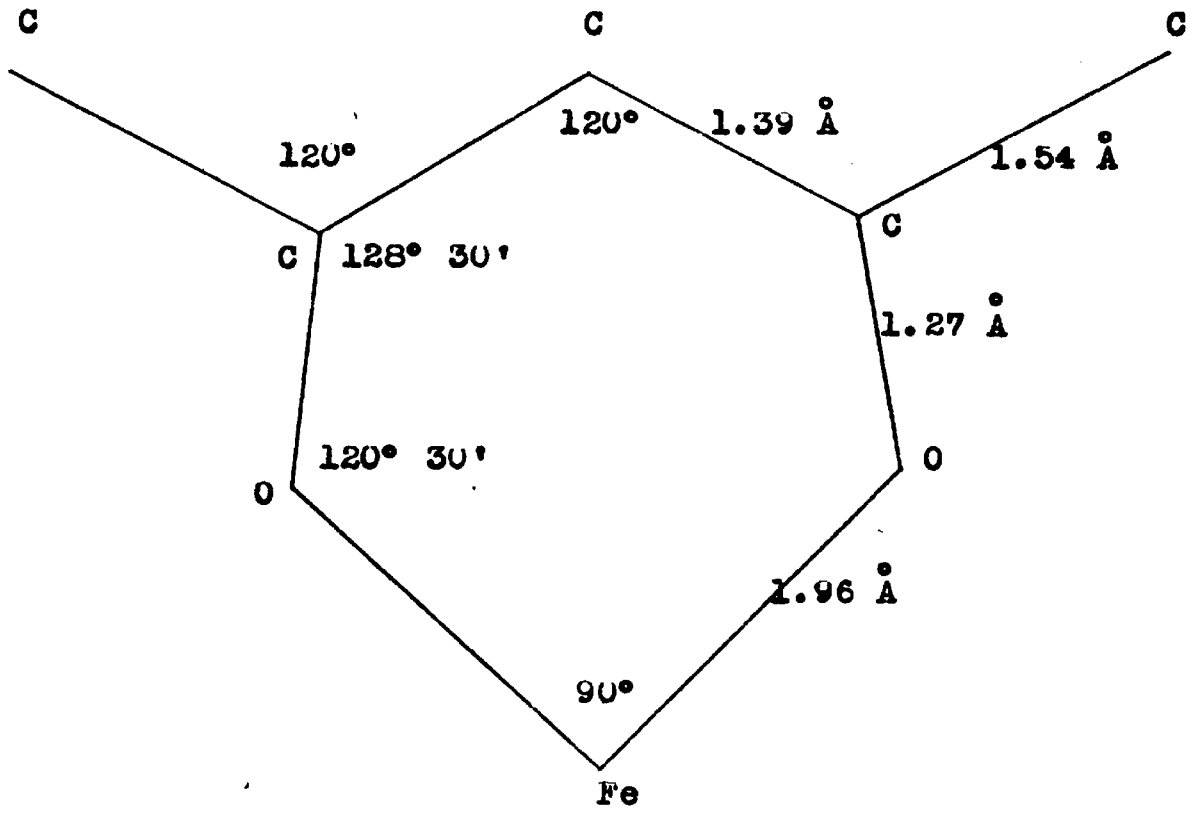


Figure 10. Ferric Acetylacetonate

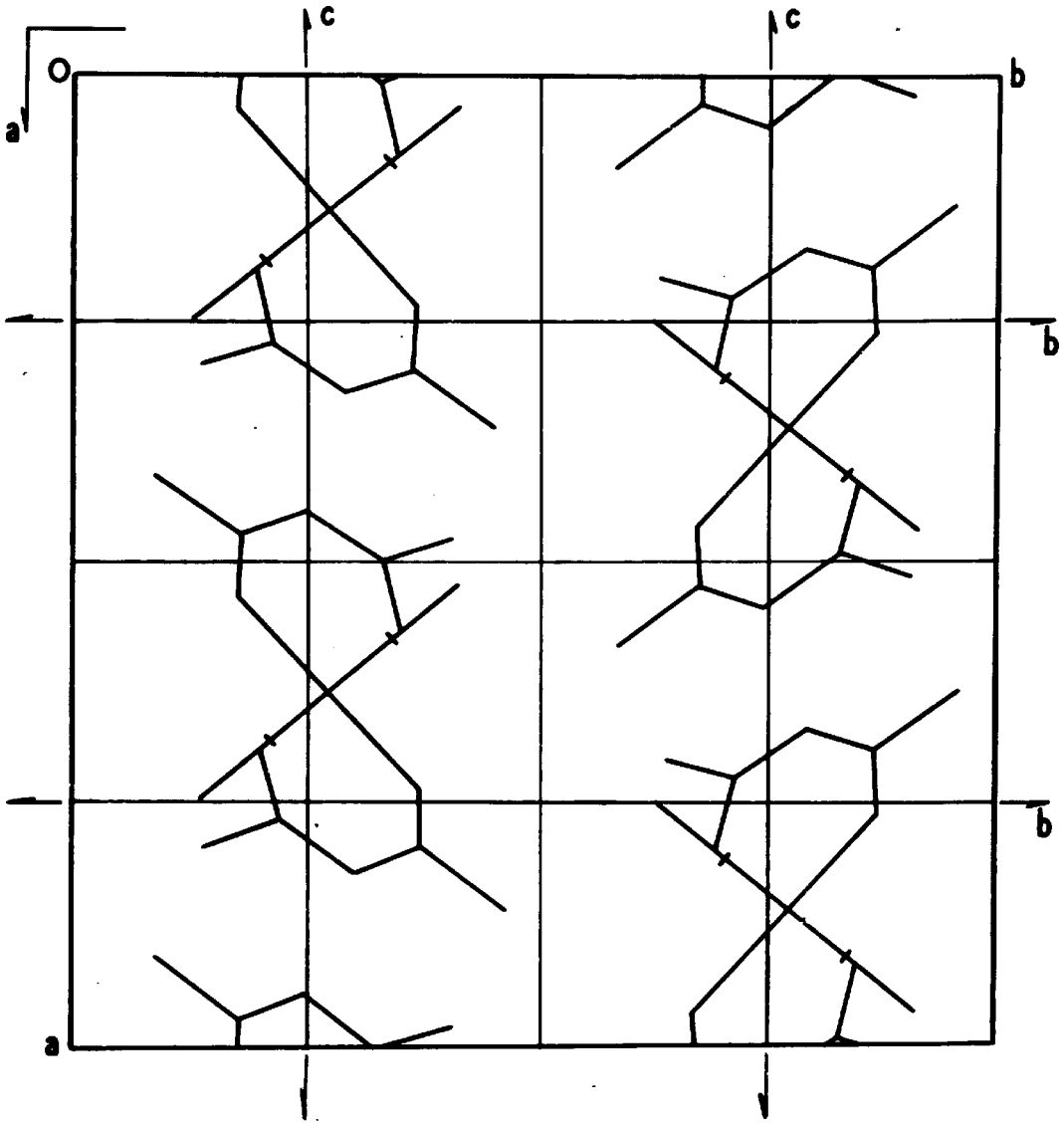


FIGURE 11 PROJECTION ON 001

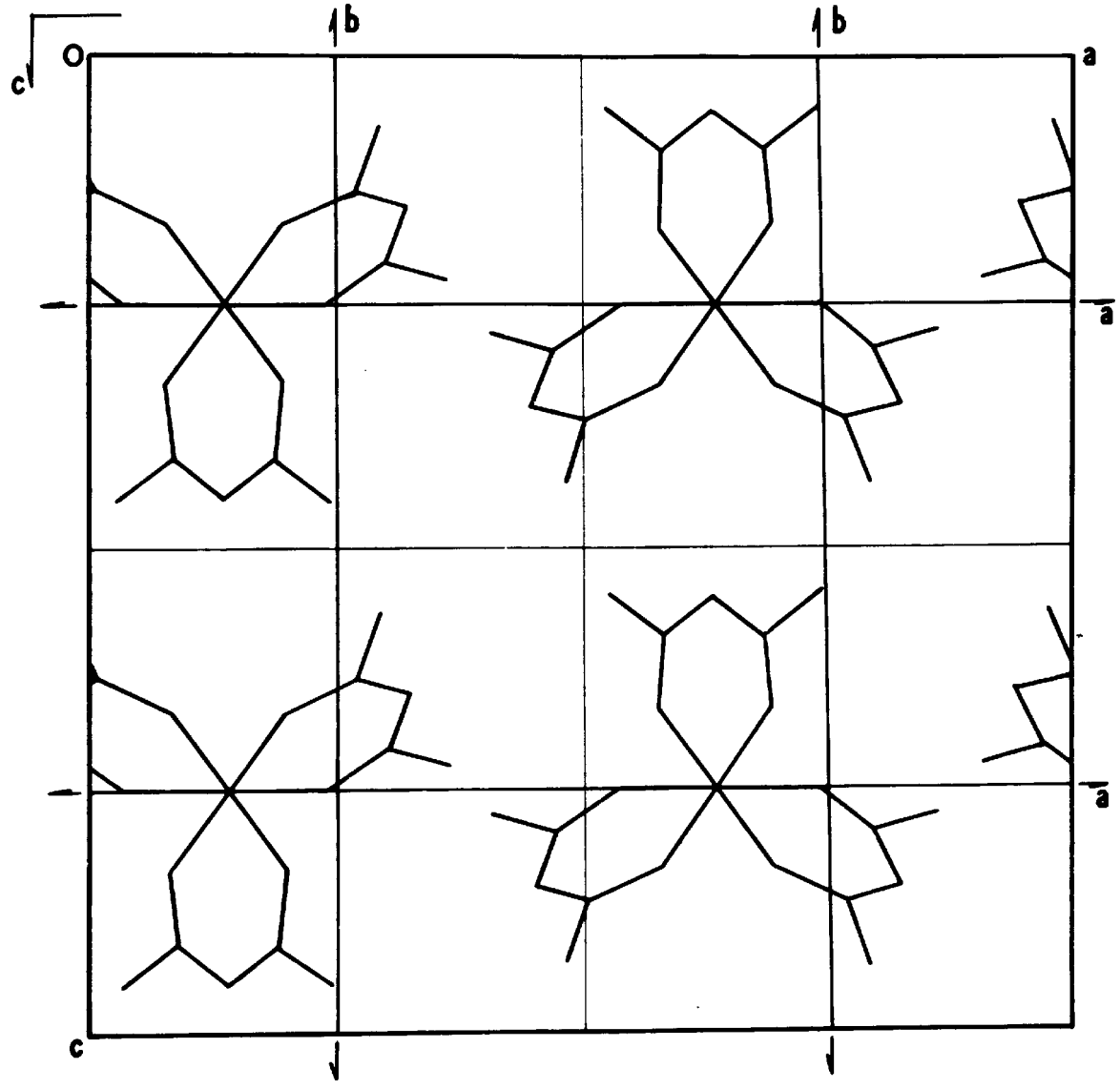


FIGURE 12 PROJECTION ON 010

Intermolecular contacts are of an order signifying very weak Van der Waals forces. The closest approach of terminal carbon atoms between molecules in the layers is 3.78 Å. for molecules related by the a glide, 4.12 Å. for molecules related by the b glide, and 5.08 Å. for molecules related by the c glide.

APPENDIX I

Observed and Calculated Structure Factors

hkλ	F_o	F_c
200	47	-32
600	14	+11
800	8	- 8
1200	20	-20
1400	22	+19
210	332	-282
410	27	+30
610	57	+53
810	4	- 6
1010	22	-15
020	316	-342
220	52	+52
620	66	-57
820	9	+12
1020	22	+13
1420	19	-12
430	73	-95
630	88	-99
830	55	+49
240	22	+21
440	95	+92
640	90	+105
840	53	+47
1040	60	-56
450	93	+108
650	85	+87
850	62	-70
1250	17	-16
260	21	+ 8
460	71	+41
660	19	-18
860	51	-67
1060	60	+38
270	12	- 5
470	24	-33
670	86	-78
870	57	+29
1270	29	-24
080	4	- 3
880	22	+23

hkλ	F_o	F_c
490	21	-39
690	35	+34
890	16	+20
0(12)0	15	+20
2(12)0	28	+28

DOUBLE REFLECTIONS

400	25	+ 5
1050	18	-53
1080	32	-23
420	68	+76
	147	157
1000	22	- 6
1220	24	+34
290	21	+ 1
	67	41
1230	18	+ 3
2100	9	-15
	27	18
040	68	+40
480	38	+14
1240	17	-41
	123	95
1440	20	+ 2
2110	23	- 3
230	77	+142
	120	147
250	30	+ 9
1070	23	+33
	53	42
060	35	+17
280	16	+19
	51	36
0(10)0	29	+ 4
1210	41	+23
	70	27
4100	23	+ 6
1030	18	+29
	41	35

hk	F_o	F_c
411	64	+64
711	8	- 5
811	24	-31
1411	16	+13
321	57	+55
421	49	-44
521	20	+19
621	21	-27
821	42	+23
1221	18	+11
131	10	- 7
231	52	-64
431	70	-61
531	42	+43
631	84	+81
1431	24	-24
241	20	-18
341	6	+ 3
441	80	+80
541	11	+10
741	43	+40
841	28	-35
1241	34	-23
151	11	-11
251	12	- 7
851	30	+31
061	18	-26
261	24	-35
461	97	-100
661	50	+39
861	28	+61
671	32	+61
871	24	-35
481	25	+34
1081	32	+39
291	50	+23
491	28	-15
891	18	+25
0101	95	+63
6101	12	+10
4111	12	+ 2
0121	65	-53
2131	28	+20

DOUBLE REFLECTIONS

hk	F_o	F_c
611	28	-18
641	16	+36
331	21	+ 3
1231	16	+37
	81	94
221	18	+ 8
211	6	+26
	24	34
271	20	- 4
2111	35	-26
	55	30
471	25	+13
451	16	+26
021	48	+69
	89	108
681	55	-26
121	8	+ 1
651	62	-94
1061	25	+34
4101	12	-23
141	12	+ 1
	174	179
3101	13	+ 2
10101	16	+22
	29	24
591	10	+ 1
1091	10	+33
	20	34
511	56	+39
841	28	-35
2101	28	- 3
	112	77

APPENDIX II

Electronic Circuits for a Microphotodensitometer

Introduction

The circuit shown in Figures 13, 14, and 15 was adapted from "Phototubes", R.C.A. Manufacturing Co., 1940, by Mr. J. L. Rooi for the measurement of very small values of illumination. The device was constructed by Mr. J. L. Rooi and the writer, and was used by the latter for the measurement of the variation in density of Weissenberg spots on photographic film.

The circuit and choice of components

This circuit can measure illuminations corresponding to phototube currents of 10^{-10} amperes. The bridge arrangement of the circuit makes the zero setting practically independent of the line voltage variations. The use of a voltage-regulated screen supply makes the sensitivity of the circuit negligibly affected by line voltage variations.

High anode voltages applied to the phototube may cause ionization of minute traces of residual gas in the tube. The gas current resulting from this ionization may produce slow changes in the tube characteristics which would change the calibration of the instrument. To overcome this effect a low anode potential is applied to the phototube, 22.5 volts. Since the current through the battery is only a few microamperes a medium-sized battery should give good life.

A high-vacuum phototube was chosen over a gas phototube for the following reasons: A high-vacuum

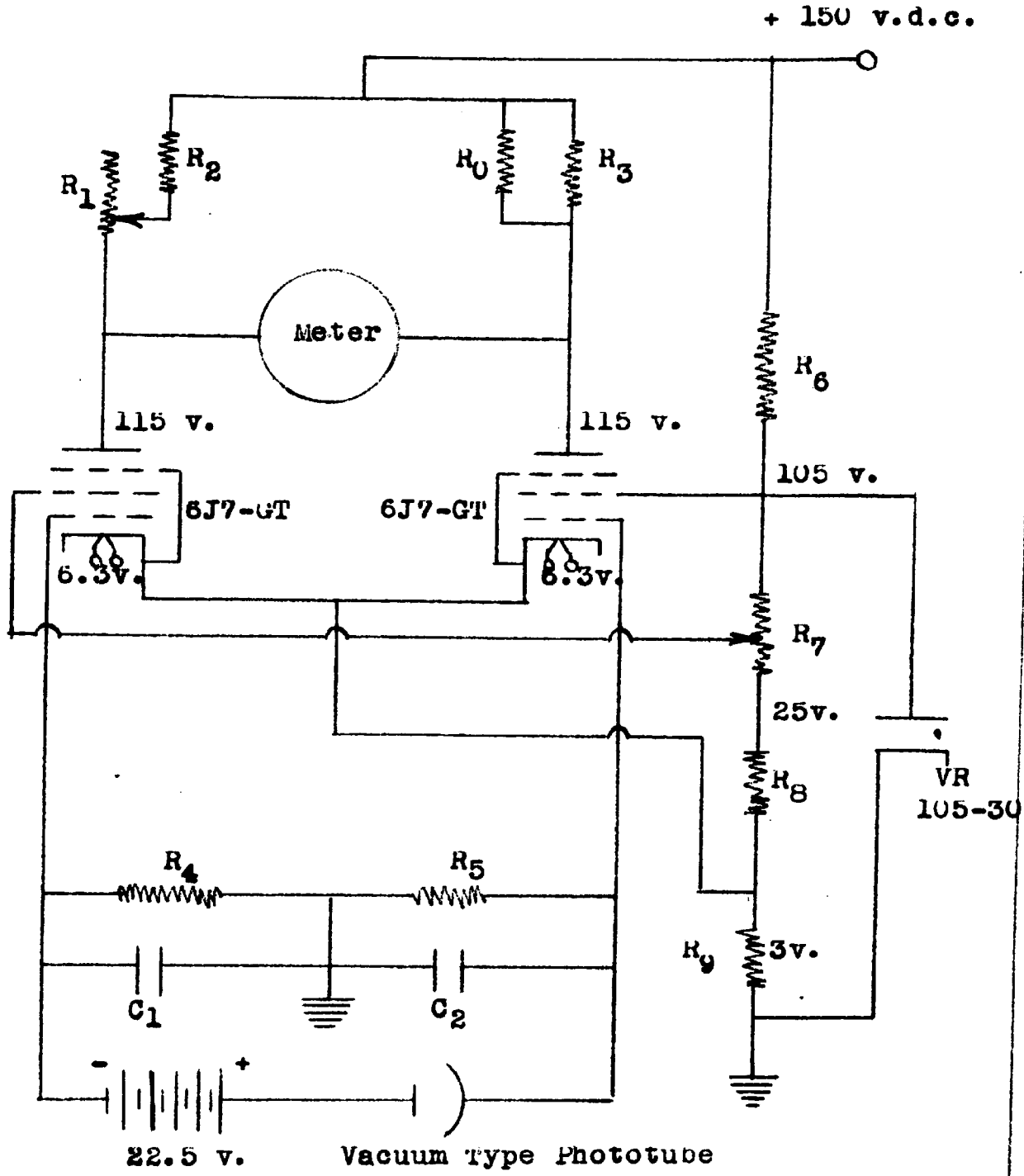


Figure 13. Circuit for Measurement of Very Small Values of Illumination

TABLE 5

Legend for Figure 13.

R_0 = adjustable (under chassis) for leakage conditions necessary to zero device

R_1 = 2000 ohm variable 1 watt

R_2 = 50,000 ohm 1 watt

R_3 = 50,000 ohm 1 watt

R_4 = 10 megohms

R_5 = 10 megohms

R_6 = 2500 ohm 2 watt

R_7 = 10,000 ohm 1 watt variable

R_8 = 2500 ohm 1 watt

R_9 = 300 ohm 1 watt

C_1 = 0.01 mfd. 400 v.

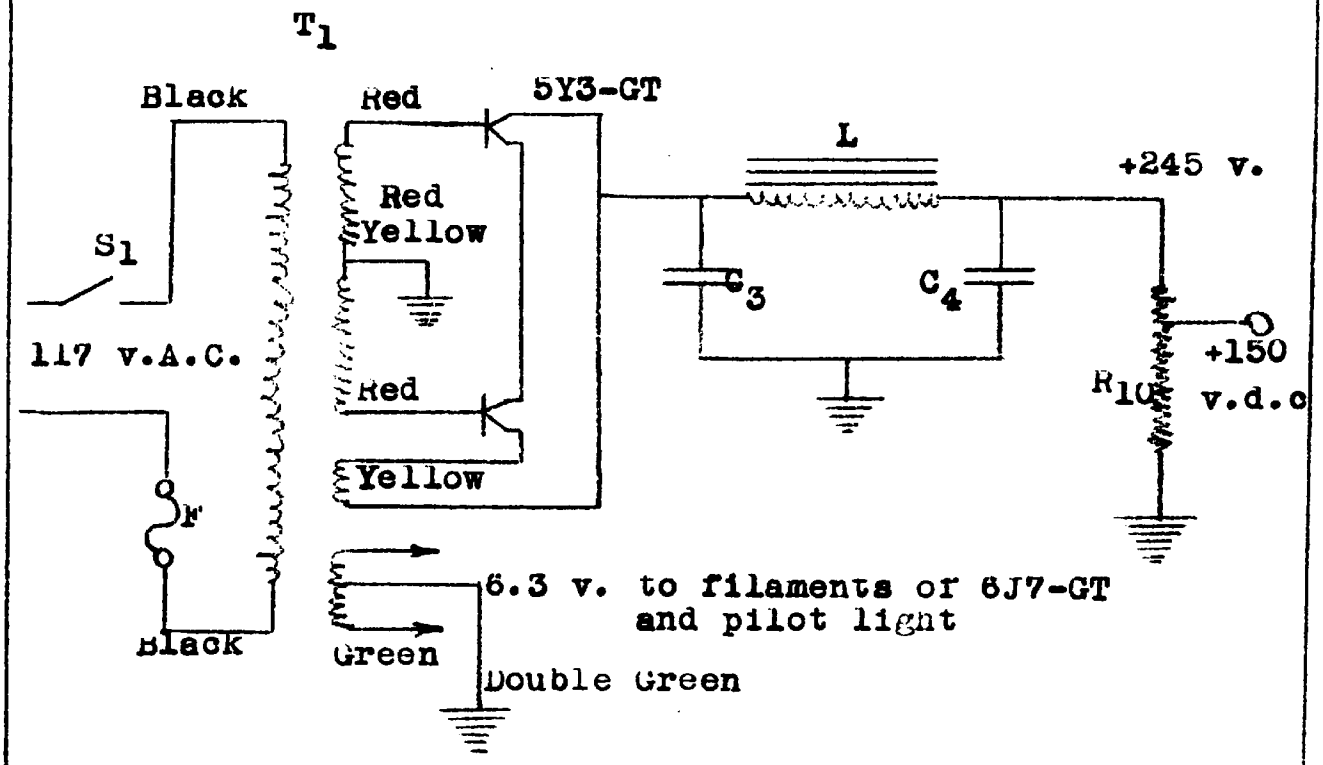
C_2 = 0.01 mfd. 400 v.

Meter = multi-range microammeter 0-25, 0-125, 0-1250

2 - 6J7-GT

1 - VR 105-30

1 - Phototube 929



S_1 = S.P.S.T. switch

F = Fuse, 1.0 amp.

R_{10} = 20,000 ohm 25 watt adjustable power resistor

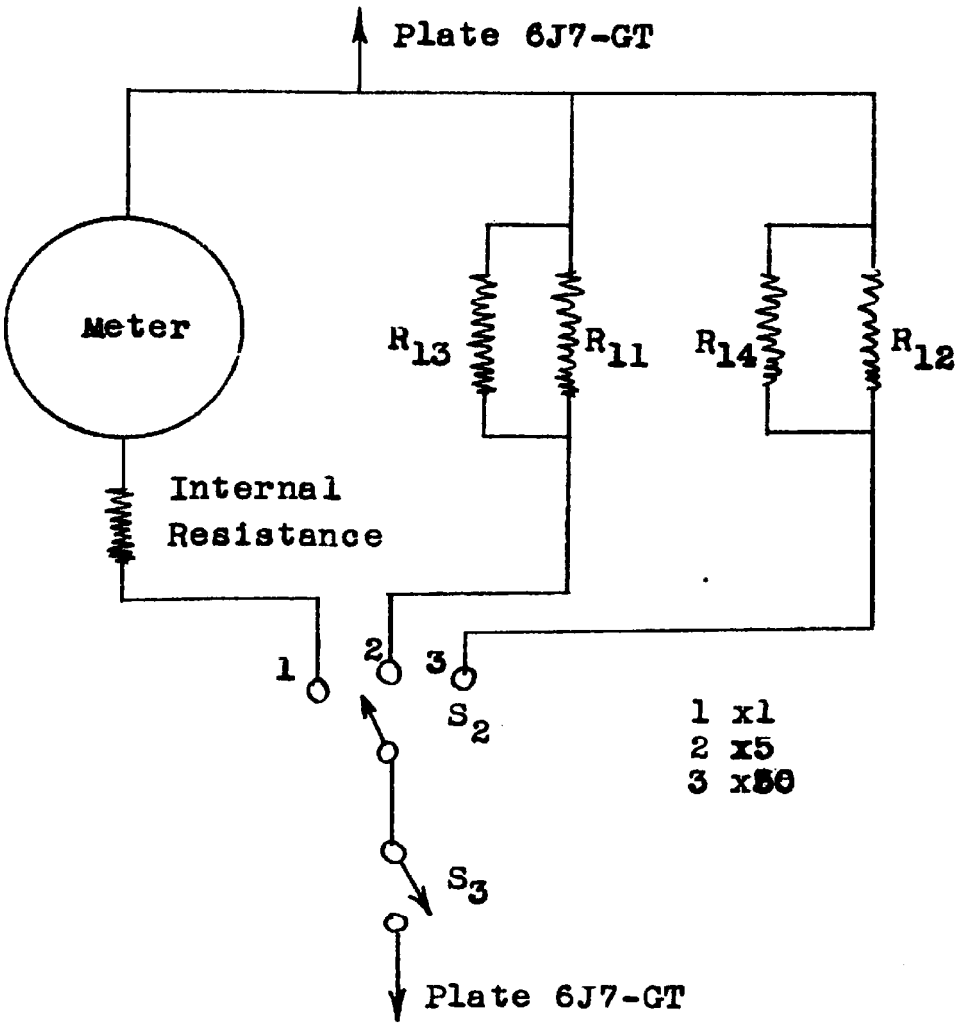
C_3, C_4 = 20-20 mfd 450 volt Electrolyte

1 - 5Y3-GT

L = Filter Choke 40 ma. Large L Stancor C1707

T_1 = Power Transformer 480 volts center tapped
5 volts at 2 amp 6.3 volts at 2 amp
Stancor PC-8401

Figure 14. Circuit for Power Supply



Internal Resistance of the Meter = 2200 ohms

S_2 = S.P. 3 Position Shorting type contacts

S_3 = S.P.S.T. (safety device for meter)

R_{11} = 550 ohms R_{12} = 45 ohms

R_{13}, R_{14} = Shunting resistance to balance unknown variation in internal resistance of meter.

Figure 15. Multiple Meter Ranges Details

phototube has more constant sensitivity throughout its life and is less likely to be damaged by accidental operation outside the limits of normal operation. A high-vacuum type is not subject to voltage breakdown and glow discharge which would ruin the sensitive material on the cathode of the phototube.

The phototube chosen was the RCA 929. This tube is more than twice as sensitive as the tube series 917, 919, and 922, which are all of the same sensitivity. The 929 has its maximum sensitivity in the blue-violet range and such light should be used; namely, a carbon arc, a mercury-vapor lamp, or a florescent lamp. Although the 929 has low red sensitivity, this type gives better sensitivity to light from an incandescent lamp than other vacuum types. A 500 watt projection-type lamp was used as the source light and gave sufficient intensity to operate the device over the meter scale when the scale was on its coarsest setting. The light from the lamp was passed through a water cell which absorbed the infra-red and prevented the light from burning holes in the film.

The grid-cap 6J7-GT was used in preference to the single-ended 6SJ7 to reduce leakage currents, which will be mentioned later.

A 0-25 microammeter was used along with shunting resistors to increase the range to 0-125 and 0-1250 micro-amperes.

In measurement circuits where the phototube must respond to very small amounts of light, phototube leakage

currents must be made small. A low-resistance leakage path (large leakage current) between the phototube terminals reduces the effective load resistance, which in turn reduces the circuit's sensitivity. Also, these leakage currents may vary erratically, and may mask the effect of the phototube current when the phototube current is small. These leakage currents can be reduced by removing dust and grease from insulating surfaces between the terminals of the phototube with a cloth dampened in alcohol.

Construction notes

The phototube itself and the leads from the phototube to the amplifier were shielded electrically. The phototube was shielded from all other light except that which the device was measuring. All components were mounted on terminal strips or tube sockets and were well insulated from each other and the chassis. The power supply bleeder resistor R_{10} was mounted above the chassis with the tubes to provide ventilation and cooling.

Calibration, Operation, Maintenance

The tap on R_{10} had to be set for 150 volts when the complete circuit was turned on and all tubes plugged in.

The procedure for adjusting the circuit was to switch the microammeter to its 0-1000 scale, reduce the phototube illumination to zero, and bring the meter reading to zero by adjustment of R_7 as a coarse control and R_1 as a fine control. The circuit was then ready for operation.

As a check on the calibration, the meter should be switched to its next lowest scale. The meter should still read zero. The device should be calibrated every time it is turned on and also during the period of service. The device was always allowed to warm up for several minutes before use.

Because the variation of meter current with illumination is practically linear, the circuit can be calibrated at comparatively large values of illumination and the calibration can be extended to small illumination values. This means that the device may be calibrated so that the meter reads a certain value, for instance 500, for a given illumination. The device would now read changes in illumination above and below the given value.

Care was also taken not to let too much light fall on the phototube while it was in the circuit and the device was working. This would cause too much current to flow through the phototube and might damage it. Exceptionally strong light was not allowed to fall on the phototube, even when it was not in the circuit, as it might decrease the sensitivity temporarily or even permanently.

A further consideration for the maintenance of constant calibration and sensitivity was that the light incident on the phototube was spread over as large a portion of the cathode surface as possible. This procedure was used to minimize variations in sensitivity that might be caused by a shift in the position of the light spot on the cathode.

BIBLIOGRAPHY

Astbury, W. T. (1926) Pro. Royal Society 112, 448.

Booth, A. D. (1948) Fourier Technique in X-ray Organic Structure Analysis. Cambridge: University Press.

Bradley, A. J. & Jay, A. H. (1932) Pro. Physical Society 44, 563.

Bragg, W. L. & Wood, E. A. (1947) American Mineralogist 32, 591.

Buerger, M. J. (1942) X-ray Crystallography, p. 221 John Wiley & Sons, Inc., New York.

Buerger, M. J. (1953) Numerical Structure Factor Tables Geological Society of America, Special Papers No. 33.

Costain, W. (1941) See Lipson & Cochran, p. 279.

Cruickshank, D. W. J. (1949) Acta Cryst. 2, 65.

Grenville-Wells, H. J., Moving-Strip Fourier Analyzer, Massachusetts Institute of Technology, Cambridge, Mass.

Harker, D. (1936) J. Chem. Phys. 4, 381.

International Tables for X-ray Crystallography (1952) Birmingham: Kynoch Press.

Internationale Tabellen zur Bestimmung von Kristallstrukturen (1935) Vol. 2, Berlin: Borntraeger.

James, R. W. (1948) The Optical Principles of the Diffraction of X-rays, p. 342, G. Bell & Sons, Ltd., London

Lipson, H. & Cochran, W. (1953) The Determination of Crystal Structures, G. Bell & Sons, Ltd., London

Morgan, G. T. (1926) Pro. Royal Society 112, 465.

Patterson, A. L. (1934) Phys. Rev. 46, 372.

Renninger, M. (1937) Z. Krist. 97, 107.

Robertson, J. M. (1936) Phil. Mag. 21, 176.

Smare, D. L. (1948) Acta Cryst. 1, 150.